Table 3. The parameters of formation water

Initial pressure (MPa)	Temperature (℃)	Salinity (mg/L)	Water formation volume factor	Types
53	152.5	13000	1.062	$NaHCO_3$

3. EXPERIMENT PROCEDURE

The first experiment was carried out in seven steps:

Step 1: The porosity and permeability of each short core were measured after selection and drying.

Step 2: The short cores were rearranged into two long cores. Filter paper was added between short cores to eliminate the tip effect. Each long core was loaded into a holder with confining pressure.

Step 3: The air was removed from each long core with the vacuum pump.

Step 4: Water was injected into the core until reaching the irreducible water saturation.

Step 5: The oven was adjusted to the in-situ temperature of 152.5 ℃, and the confining pressure of the long core was set to the formation pressure of 53 MPa.

Step 6: The pressure was changed by adjusting the inlet pressure and the backpressure valve. The pressure in the long core was reduced to 1MPa with a step length of 3MPa. The outlet flow rate, time, inlet pressure and outlet pressure were recorded in real time. The water vessel was connected to the inlet to simulate the impact of aquifer.

Step 7: The core was cleaned with ether and dried in nitrogen.

The second experiment was conducted by repeating the Steps 3~6 to simulate the impact of different aquifer volumes.

4. EXPERIMENTAL RESULTS

4.1 Well DF-Z-2

The short cores from well DF-Z-2 were used to simulate the depletion production of gas reservoir without aquifer with long-core displacement. The PIC and the cumulative gas production of the well are shown in Figure 2 and Table 4, respectively. It can be seen that the PIC of AHP gas reservoir without aquifer was basically a straight line, rather than the traditionally believed curve with sectional downward bend.

Table 4. Cumulative gas production of Well DF-Z-2

Pressure (MPa)	53	50	47	44	41	38	35	32	29
Cumulative gas production (cm^3)	0	177.3	205.4	223.2	241.9	261.5	279.3	303.1	329.5
Pressure (MPa)	26	23	20	17	14	11	8	5	1
Cumulative gas production (cm^3)	356.3	365.2	385.6	405.1	438.3	468.0	510.1	533.5	576.5

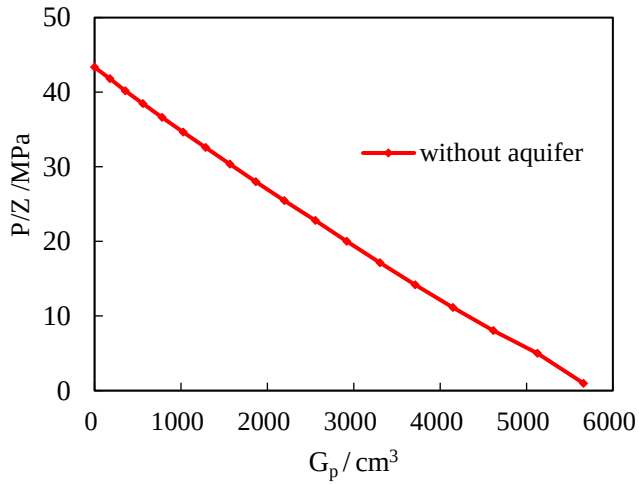

Figure 2. The PIC of Well DF-Z-2

4.2 Well DF-Z-8D

The short cores from Well DF-Z-8d were used to simulate the depletion production of gas reservoir with finite aquifer in different volumes. Table 5 lists the cumulative gas productions of different finite aquifers: (1) With the same porosity, the cumulative gas production increased slightly with the growth in aquifer volume; (2)The aquifer volume is positively correlated with the initial gas production rate, and negatively with the later gas production rate; (3) The gas production rate plunged after water breakthrough.

Table 5. Cumulative gas productions of Well DF-Z-8d with different aquifer volumes

Pressure (MPa)	Cumulative gas production (cm^3)			
	5 PV volume	10 PV volume	20 PV volume	50 PV volume
53	0.0	0.0	0.0	0.0
50	592.2	714.8	837.3	1079.1
47	1180.2	1415.3	1649.2	2090.2
44	1766.4	2103.7	2437.8	3060.7
41	2350.1	2777.9	3197.0	3964.7
38	2930.7	3436.3	3929.2	4825.9
35	3507.5	4076.6	4626.4	5620.0
32	4079.5	4698.1	5293.5	6367.2
29	4645.4	5296.8	5921.6	7048.3
26	5203.8	5870.2	6504.9	7653.3
23	5752.1	6416.5	7048.6	8194.8
20	6287.3	6929.2	7539.1	8642.0
17	6807.0	7407.4	7989.4	9019.2
14	7307.4	7844.4	8366.9	9073.8
11	7781.2	8234.8	8676.1	9116.8
8	8221.7	8578.0	8920.9	9152.2
5	8624.0	8862.3	9094.5	9182.4
1	9084.7	9139.6	9191.1	9216.9

As shown in Figure 3 and Table 6, the cumulative water production (W_p) and cumulative gas production (G_p) exhibited the following trends: (1) No water was produced in the well with the 5PV (pore volume) aquifer or with the 10PV aquifer; (2) Water production started when the aquifer volume increased to 20PV; (3) More water was produced when the aquifer volume grew to 50PV, which happened in the late

period of depletion production, while the PIC of the gas reservoir started to bend downward.

Table 6. Cumulative water fluxes of Well DF-Z-8d with different aquifer volumes

Pressure (MPa)	Cumulative water production (cm^3)			
	5 PV volume	10 PV volume	20 PV volume	50 PV volume
53	0.0	0.0	0.0	0.0
50	0.0	0.0	0.0	0.0
47	0.0	0.0	0.0	0.0
44	0.0	0.0	0.0	0.0
41	0.0	0.0	0.0	0.0
38	0.0	0.0	0.0	0.0
35	0.0	0.0	0.0	0.0
32	0.0	0.0	0.0	0.0
29	0.0	0.0	0.0	0.0
26	0.0	0.0	0.0	0.0
23	0.0	0.0	0.0	0.0
20	0.0	0.0	0.0	0.0
17	0.0	0.0	0.0	0.0
14	0.0	0.0	0.0	2.3
11	0.0	0.0	0.0	4.8
8	0.0	0.0	0.0	7.5
5	0.0	0.0	0.0	10.3
1	0.0	0.0	0.3	13.6

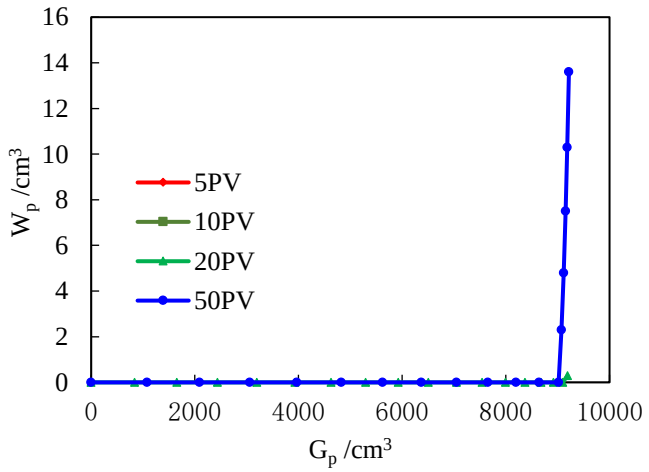

Figure 3. Water productions of Well DF-Z-8d with different aquifer volumes

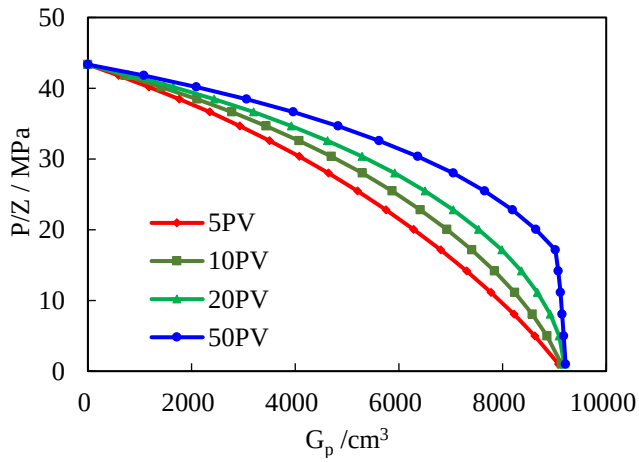

Figure 4. The PICs of Well DF-Z-8d

The following can be derived from the PICs in Figure 4: (1) The PIC of water-drive gas reservoir is generally a smooth convex, which eventually intersects the cumulative gas axis at the dynamic OGIP point; (2) The PIC convexity is positively correlated with aquifer volume; (3) When the aquifer volume reached 50PV, the production index curve bent abruptly downward to the point of dynamic OGIP at the end period because of water production.

5. DISCUSSION

It can be seen from Figures 2 and 4 that, the PIC of AHP gas reservoir is a smooth convex [8-10,18], not the traditionally believed curve with sectional downward bend [6, 7]. If the aquifer is finite, the PIC of AHP gas reservoir exists as a smooth convex curve; if the aquifer is absent, the PIC takes the shape of a straight line.

Moreover, piston-like displacement features were observed in the simulations of depletion production with long-core displacement [4]. The larger the aquifer, the more the energy retained in the gas reservoir, and the higher the recovery ratio at the same abandonment pressure.

Owing to the heterogenous terrain and imbalanced production, water breakthrough will occur earlier in actual gas reservoir. After water breakthrough, the critical time in the PIC will shift counterclockwise towards gas recovery reduction. The water breakthrough will magnify the features of terrain heterogeneity and production imbalance. In this case, the recovery ratio will decrease with the growth in the abandonment pressure.

To push up the recovery ratio, balanced development should be pursued in water-drive gas reservoir to ensure stable uplift of gas-water contact.

6. CONCLUSIONS

Through simulations of depletion production with long-core displacement, it is concluded that the PIC of water-drive gas reservoir is generally a smooth convex, which eventually intersects the cumulative gas axis at the dynamic OGIP point; The PIC convexity is positively correlated with aquifer volume. The results confirm that the AHP gas reservoir is a special gas reservoir with finite aquifer, and the traditionally view that the PIC of the AHP gas reservoir with sectional downward bend is incorrect.

Moreover, piston-like displacement features were observed in the simulations of depletion production with long-core displacement. The larger the aquifer, the more the energy retained in the gas reservoir, and the higher the recovery ratio at the same abandonment pressure. To push up the recovery ratio, balanced development should be pursued in water-drive gas reservoir to ensure stable uplift of gas-water contact.

ACKNOWLEDGMENT

This paper is supported by the National Science and Technology Major Project of China (2016ZX05024005) and the Comprehensive Scientific Research Projects of CNOOC (YXKY-2016-ZHJ-02).

REFERENCES

[1] Li, C.L. (2011). Fundamentals of reservoir engineering. Beijing: Petroleum Industry Press, 124-183.

[2] Zhang, L.Y., Li, J. (1998). Curve fitting method of dynamic reserve calculation in water driver gas reservoir. Natural Gas Industry, 18(2): 26-29.

[3] Ahmed, T. (2001). Reservoir engineering handbook. Gulf Professional Publishing.

[4] John, L., Robert, A.W. (1996). Gas reservoir engineering. Henry L. Doherty Memorial Fund of AIME, Society of Petroleum Engineers.

[5] Dake, L.P. (1978). Fundamentals of reservoir engineering. Amsterdam, Elsevier.

[6] Ezekwe, N. (2010). Petroleum reservoir engineering practice. Prentice Hall.

[7] Hammerlindl, D.J. (1971). Predicting gas reservoirs in abnormally pressured reservoirs. SPE 3479.

[8] Li, C.L. (2007). Misunderstanding the performance of abnormal pressure gas reservoir. Journal of Southwest Petroleum University, 29(2): 166-169.

[9] Yang, C.Q., Peng, X.D., Wang, X.G., Luo, J., Tong, L.Y. (2017). New understanding on production index curve of water drive gas reservoir: a case study of north block in YC13-1 gas field. China Offshore Oil and Gas, 29(1): 77-82.

[10] Peng, X.D., Zhu, S.P., Wang, Q.S., Luo, J., Lu, Y. (2018). New calculation method of dynamic OGIP and aquifer volume in gas reservoirs with restricted and closed aquifers. China Offshore Oil and Gas, 30(2): 77-82.

[11] Zhu, H.Y., Yu, X.H., Wan, Y.J. (2003). Simulation experiment of depletion drive development for anomaly high pressure gas reservoir of KeLa 2 gas field. Natural Gas Industry, 23(4): 62-64.

[12] Jiang, G.J., Tang, S.S., Huang, Y.H., Zhou, Y.Z. (2013). A depletion experimental study of carbonate sour gas reservoirs. Petrochemical Industry Application, 32(1): 60-63.

[13] Jiao, C.Y., Zhu, H.Y., Hu, Y., Xu, X. (2014). The physical experiment and numerical model of water invasion to the gas reservoir. Science Technolog and Engineering, 14(10): 191-194.

[14] He, M.Y., Sun, C.X., Xu, B.W., Qi, L.S. (2017). Experimental study on influence of gas recovery rate on production performance in gas fields. Contemporary Chemical Industry, 46(3): 454-456.

[15] Xie, Y.H. (2016). Hydrocarbon accumulation mechanism and resource prospect of HTHP natural gas reservoirs in Western South China Sea: A case study on the Ying-Qiong Basin. Oil Drilling & Production Technology, 38(6): 713-722.

[16] Zhang, H.L., Pei, J.X., Zhang, Y.Z., Jiang, C.Y., Zhu, J.C., Ai, N.P., Hu, Q.W., Yu, J.F. (2013). Overpressure reservoirs in the mid-deep Huangliu Formation of the Dongfang area, Yinggehai Basin, South China Sea. Petroleum Exploration and Development, 40(3): 284-293.

[17] Huang, Z.L., Zhu, J.C., Ma, J., Wu, H.Z, Zhang, H.L. (2015). Characteristics and genesis of high-porosity and low-permeability reservoirs in the Huangliu Formation of high temperature and high pressure zone in Dongfang area, Yinggehai Basin. Oil & Gas Geology, 36(2): 288-295.

[18] Fetkovich, M.J., Reese, D.E., Whitton, C.H. (1998). Application of a general material balance for high-pressure gas reservoirs. SPE22921, 3-13.